

Spin-density matrix elements in hard exclusive muoproduction of ω mesons at COMPASS

B.Marianski^{*†}

for the COMPASS Collaboration

National Centre for Nuclear Research Warsaw

E-mail: b.marianski@ncbj.gov.pl

Spin density matrix elements (SDMEs) have been determined for exclusive ω meson production on unpolarized protons, in the COMPASS kinematic region of $1.0 (\text{GeV}/c)^2 < Q^2 < 10.0 (\text{GeV}/c)^2$, $5.0 \text{ GeV}/c^2 < W < 17.0 \text{ GeV}/c^2$ and $0.01 (\text{GeV}/c)^2 < p_T^2 < 0.5 (\text{GeV}/c)^2$ which corresponds to $\langle Q^2 \rangle = 2.1 (\text{GeV}/c)^2$, $\langle W \rangle = 7.6 \text{ GeV}/c^2$ and $\langle p_T^2 \rangle = 0.16 (\text{GeV}/c)^2$ mean values. Using extracted SDMEs values the contribution of unnatural parity exchange amplitudes and the hypothesis of s-channel helicity conservation (SCHC) were studied. Certain matrix elements e.g. r_{00}^5 corresponding to transition $\gamma_T^* \rightarrow V_L$ indicate violation of SCHC in exclusive ω production. A sizable contribution of unnatural parity exchange amplitudes is found for the exclusive ω meson muoproduction, and there is a clear indication of its decrease with increasing W .

*23rd International Spin Physics Symposium - SPIN2018 -
10-14 September, 2018
Ferrara, Italy*

^{*}Speaker.

[†]Work supported by the NCN Grant 2017/26/M/ST2/00498

1. Definition of Spin Density Matrix Elements

Study of exclusive muoproduction of vector mesons allows investigation of both production mechanism and structure of the nucleon. In particular it gives the possibility to constrain Generalized Parton Distribution (GPDs). At leading twist the chiral-even GPDs $H^{q(g)}(x, \xi, t)$, $E^{q(g)}(x, \xi, t)$, $\tilde{H}^{q(g)}(x, \xi, t)$, $\tilde{E}^{q(g)}(x, \xi, t)$ with helicity of parton unchanged describe exclusive vector meson production on spin 1/2 target. When higher twist effects are included in the distribution amplitude, chiral odd GPDs $H_T^{q(g)}(x, \xi, t)$, $E_T^{q(g)}(x, \xi, t)$, $\tilde{H}_T^{q(g)}(x, \xi, t)$, $\tilde{E}_T^{q(g)}(x, \xi, t)$ with parton helicity flip, appear.

Angular distribution of the decaying particles from vector meson depends on vector meson Spin Density Matrix Elements (SDMEs). These elements on the other hands, are bilinear combination of helicity amplitudes $F_{\lambda_V \lambda'_V \lambda_\gamma \lambda_N}$, where λ_γ is a virtual photon helicity and λ_V vector meson helicity, while λ_N and λ'_N are the helicities of the nucleon in the initial and final states, respectively.

In the γ^*N centre-of-mass (CM) system the spin density matrix of the vector meson is given by the von Neumann equation [1],

$$\rho_{\lambda_V \lambda'_V} = \frac{1}{2\mathcal{N}} \sum_{\lambda_\gamma \lambda'_N \lambda_N} F_{\lambda_V \lambda'_N \lambda_\gamma \lambda_N} \rho_{\lambda_\gamma \lambda'_\gamma}^{U+L} F_{\lambda'_V \lambda'_N \lambda'_\gamma \lambda'_N}^* \quad (1.1)$$

where \mathcal{N} is a normalization factor [1, 2] and $\rho_{\lambda_\gamma \lambda'_\gamma}^{U+L}$ is the virtual photon spin density matrix, where U and L denote unpolarized and longitudinally polarized beam, respectively [2].

After the decomposition of $\rho_{\lambda_\gamma \lambda'_\gamma}^{U+L}$ into the standard set of 3×3 Hermitian matrices Σ^α , the vector-meson spin density matrix is expressed in terms of a set of nine matrices $\rho_{\lambda_V \lambda'_V}^\alpha$ related to various photon polarization states: transversely polarized photon ($\alpha=0, \dots, 3$), longitudinally polarized photon ($\alpha=4$), and terms describing their interference ($\alpha=5, \dots, 8$) [1]. In case when contributions of transverse and longitudinal photons cannot be separated, the SDMEs are customarily defined as

$$r_{\lambda_V \lambda'_V}^{04} = (\rho_{\lambda_V \lambda'_V}^0 + \varepsilon R \rho_{\lambda_V \lambda'_V}^4) (1 + \varepsilon R)^{-1},$$

$$r_{\lambda_V \lambda'_V}^\alpha = \begin{cases} \rho_{\lambda_V \lambda'_V}^\alpha (1 + \varepsilon R)^{-1}, & \alpha = 1, 2, 3, \\ \sqrt{R} \rho_{\lambda_V \lambda'_V}^\alpha (1 + \varepsilon R)^{-1}, & \alpha = 5, 6, 7, 8. \end{cases} \quad (1.2)$$

The quantity $R = d\sigma_L/d\sigma_T$ is the longitudinal-to-transverse virtual-photon differential cross-section ratio and ε is the virtual photon polarisation parameter.

The helicity amplitudes are decomposed into the sum of the amplitudes T for natural-parity exchange (NPE) ($P=(-1)^J$) and the amplitudes U for unnatural-parity exchange (UPE) ($P=-(-1)^J$), hence given by $F_{\lambda_V \lambda'_N, \lambda_\gamma \lambda_N} = T_{\lambda_V \lambda'_N, \lambda_\gamma \lambda_N} + U_{\lambda_V \lambda'_N, \lambda_\gamma \lambda_N}$. For an unpolarized target there is no interference between NPE and UPE. Also for an unpolarized target there is no linear contribution of nucleon-helicity-flip amplitudes to SDMEs. Bilinear contributions of nucleon helicity flip amplitudes are neglected as they are suppressed by a factor $(\frac{\sqrt{-t'}}{M})^2$, where t' is a measure of the transverse momentum of the vector meson with respect to the direction of the virtual photon. So it is convenient to use the following abbreviation $T_{\lambda_V \lambda_\gamma} \equiv T_{\lambda_V \frac{1}{2} \lambda_\gamma \frac{1}{2}}$. This reduces the number of amplitudes to nine: the helicity conserving amplitudes T_{00}, T_{11}, U_{11} , and the helicity non-conserving amplitudes $T_{01}, T_{10}, T_{1-1}, U_{01}, U_{10}, U_{1-1}$. The dominance of diagonal transitions is called s-channel helicity conservation (SCHC).

interval $-3.0 \text{ GeV} < E_{\text{miss}} < 3.0 \text{ GeV}$. In Fig. 1 the missing energy distribution is shown by the red histogram. Blue dashed area corresponds to E_{miss} distribution for the LEPTO MC simulation reweighted in the same way as in Ref. [3]. The fraction of background for the entire kinematic region is 20%. In Fig. 2 invariant mass of $\gamma\gamma$ and distributions of $\pi^+\pi^-\pi^0$ invariant mass are shown. After all cuts we have 3060 exclusive events.

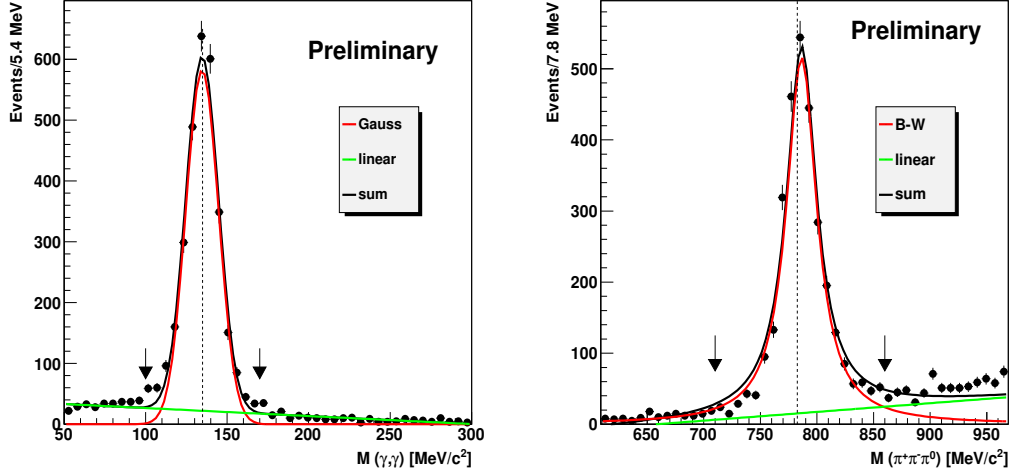


Figure 2: Left panel: Distributions of $\gamma\gamma$ invariant mass (left) fitted by Gaussian function and linear background. Dashed vertical line denotes PDG value. Right panel: Distributions of $\pi^+\pi^-\pi^0$ invariant mass (right) fitted by Breit-Wigner function and linear background. Vertical arrows denote cuts for the invariant mass. Dashed vertical line denotes PDG value.

3. Test of the SCHC Hypothesis

The SDMEs for the entire kinematic region have been determined in the COMPASS kinematic region of $1.0 \text{ (GeV/c)}^2 < Q^2 < 10.0 \text{ (GeV/c)}^2$, $5.0 \text{ GeV/c}^2 < W < 17.0 \text{ GeV/c}^2$ and $0.01 \text{ (GeV/c)}^2 < p_T^2 < 0.5 \text{ (GeV/c)}^2$, which corresponds to $\langle Q^2 \rangle = 2.1 \text{ (GeV/c)}^2$, $\langle W \rangle = 7.6 \text{ GeV/c}^2$ and $\langle p_T^2 \rangle = 0.16 \text{ (GeV/c)}^2$. Here, Q^2 represents the negative-square of the virtual-photon four-momentum, W the invariant mass of the photon-nucleon system and p_T^2 the squared transverse momentum of ω with respect to virtual photon γ^* . The SDMEs of the ω meson for the integrated data are presented in Fig. 3. The presented SDMEs are divided into five classes corresponding to different helicity transitions. Class A corresponds to the transition of longitudinal virtual photons to longitudinal mesons $\gamma_L^* \rightarrow V_L$ and transverse virtual photons to transverse mesons $\gamma_T^* \rightarrow V_T$. Class B corresponds to the interference of these two transitions. Class C corresponds to the $\gamma_T^* \rightarrow V_L$ transition, class D to the $\gamma_L^* \rightarrow V_T$ transition, and class E to the $\gamma_T^* \rightarrow V_{-T}$ transition.

In the case of SCHC only the seven SDMEs of class A and class B (r_{00}^{04} , r_{1-1}^1 , $\text{Im}\{r_{1-1}^2\}$, $\text{Re}\{r_{10}^5\}$, $\text{Im}\{r_{10}^6\}$, $\text{Im}\{r_{10}^7\}$, $\text{Re}\{r_{10}^8\}$), are not restricted to be zero, but six of them have to obey the following relations [1]: $r_{1-1}^1 = -\text{Im}\{r_{1-1}^2\}$, $\text{Re}\{r_{10}^5\} = -\text{Im}\{r_{10}^6\}$, $\text{Im}\{r_{10}^7\} = \text{Re}\{r_{10}^8\}$.

For these SDMEs we found: $r_{1-1}^1 + \text{Im}\{r_{1-1}^2\} = -0.01 \pm 0.038 \pm 0.047$, $\text{Re}\{r_{10}^5\} + \text{Im}\{r_{10}^6\} = 0.044 \pm 0.011 \pm 0.013$, $\text{Im}\{r_{10}^7\} - \text{Re}\{r_{10}^8\} = -0.088 \pm 0.110 \pm 0.196$.

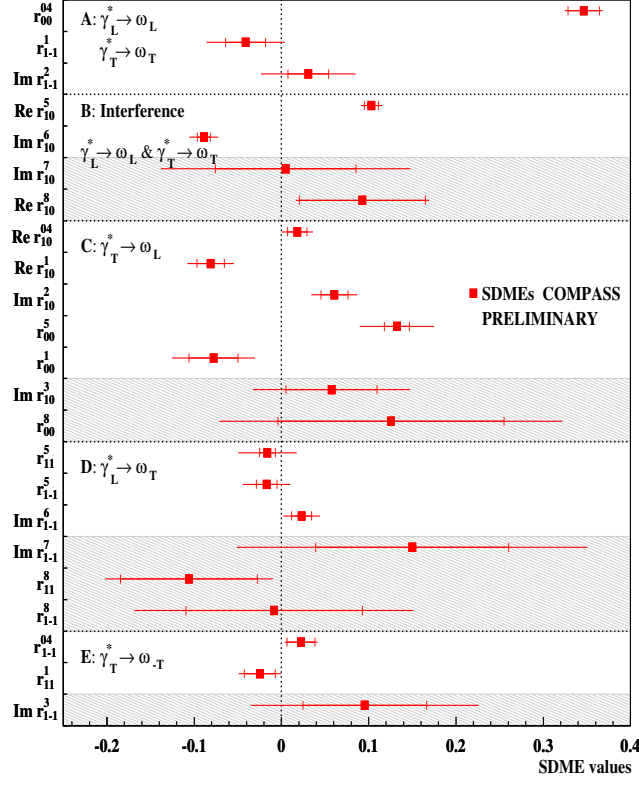


Figure 3: The 23 SDMEs extracted for exclusive ω production in the entire COMPASS kinematic region with $\langle Q^2 \rangle = 2.1 \text{ (GeV/c}^2\text{)}$, $\langle W \rangle = 7.6 \text{ GeV/c}^2$ and $\langle p_T^2 \rangle = 0.16 \text{ (GeV/c}^2\text{)}$ mean values. The inner error bars represent the statistical uncertainties, while the outer ones indicate the statistical and systematic uncertainties added in quadrature. SDMEs measured with unpolarized (polarized) beam are displayed in the unshaded (shaded) areas.

These relations for classes A and B fulfill the requirements of SCHC. All other SDMEs are required by SCHC to be zero. However, from Fig. 3 one can see that few SDMEs of class C, like $\text{Re } r_{00}^5$, $\text{Re } r_{10}^1$, $\text{Im } r_{10}^2$, are inconsistent with the hypothesis of SCHC.

4. Dependence of selected SDMEs on W

Beside of SDMEs for the entire kinematic region, the kinematic dependences of SDMEs on Q^2 , p_T^2 and W were also determined. In Table 1 values of SDMEs r_{1-1}^1 and $\text{Im } r_{1-1}^2$ as a function of $\langle W \rangle$ are shown. The difference between these two SDMEs expressed by helicity amplitudes is the following:

Table 1: Dependence of SDMEs r_{1-1}^1 , $\text{Im}r_{1-1}^2$ and u_1 on W

$\langle W \rangle$ (GeV/c ²)	5.9	7.1	9.9
r_{1-1}^1	$-0.134 \pm 0.043 \pm 0.32$	$-0.044 \pm 0.036 \pm 0.33$	$0.052 \pm 0.038 \pm 0.047$
$\text{Im}r_{1-1}^2$	$0.139 \pm 0.044 \pm 0.46$	$0.037 \pm 0.036 \pm 0.24$	$-0.098 \pm 0.038 \pm 0.033$
u_1	$1.05 \pm 0.14 \pm 0.039$	$0.90 \pm 0.12 \pm 0.021$	$0.60 \pm 0.11 \pm 0.12$

$$\text{Im}\{r_{1-1}^2\} - r_{1-1}^1 = \frac{1}{\mathcal{N}} (-|T_{\frac{1}{2}\frac{1}{2}}|^2 - |T_{1-\frac{1}{2}\frac{1}{2}}|^2 + |U_{\frac{1}{2}\frac{1}{2}}|^2 + |U_{1-\frac{1}{2}\frac{1}{2}}|^2). \quad (4.1)$$

Where \mathcal{N} is a normalization factor [4]. As mentioned in the first section $T_{1-\frac{1}{2}\frac{1}{2}}$, $U_{1-\frac{1}{2}\frac{1}{2}}$, amplitudes corresponding to nucleon helicity spin flip are suppressed and can be omitted. Using the abbreviation introduced in the first section we get

$$\text{Im}\{r_{1-1}^2\} - r_{1-1}^1 = \frac{1}{\mathcal{N}} (-|T_{\frac{1}{2}\frac{1}{2}}|^2 + |U_{\frac{1}{2}\frac{1}{2}}|^2) = \frac{1}{\mathcal{N}} (-|T_{11}|^2 + |U_{11}|^2). \quad (4.2)$$

From Table 1 one can see that for $\langle W \rangle = 5.9$ GeV/c², $\langle p_T^2 \rangle = 0.16$ (GeV/c)² the difference of the SDMEs is large and positive ($\text{Im}r_{1-1}^2 - r_{1-1}^1 > 0 \Rightarrow U_{11} > T_{11}$) so the unnatural parity amplitude is greater than natural parity one.

For $\langle W \rangle = 7.1$ GeV/c², $\langle p_T^2 \rangle = 0.16$ (GeV/c)² the values of SDMEs are close to zero and their difference is also close to zero ($\text{Im}r_{1-1}^2 - r_{1-1}^1 \approx 0 \Rightarrow U_{11} \approx T_{11}$) and the NPE amplitude is almost equal to the UPE amplitude.

For $\langle W \rangle = 9.9$ GeV/c², $\langle p_T^2 \rangle = 0.16$ (GeV/c)² one observe that the SDMEs reverse the signs, which indicate that $r_{1-1}^2 - r_{1-1}^1 \leq 0 \Rightarrow U_{11} \leq T_{11}$. The UPE processes become smaller than NPE ones. It is consistent with expectation that the fractional contribution of UPE (e.g. pion exchange) decreases as W increases.

This is also confirmed by the W dependence of the parameter u_1 which is a measure of UPE contribution, defined as $u_1 = 1 - r_{00}^0 + 2r_{1-1}^0 - 2r_{11}^1 - 2r_{1-1}^1$. It can be expressed by the helicity amplitudes $u_1 = \frac{\sum 4\epsilon|U_{10}|^2 + 2|U_{11} + U_{-11}|^2}{\mathcal{N}}$. The numerator of u_1 depends only on UPE amplitudes, thus $u_1 > 0$ is a signal of UPE contribution. We see from the fourth row of Table 1 that the UPE contribution decreases with increasing W but it is still large as $|U_{11}|$ is comparable with $|T_{11}|$.

References

- [1] K. Schilling and G. Wolf, *Nucl. Phys. C* **61** (361) 1973
- [2] A. Airapetian et al. (HERMES Collaboration), *Eur. Phys. J. C* **62** (659) 2009
- [3] COMPASS Collaboration, *Nucl. Phys. B* **915** (454) 2017
- [4] A. Airapetian et al., (HERMES Collaboration), *Eur. Phys. J. C* **74**, 3110 (2014); Erratum: *Eur. Phys. J. C* **76**, 162 (2016).